24th COBEM - 2017

24th ABCM International Congress of Mechanical Engineering
December 3-8, 2017, Curitiba, PR, Brazil

COBEM-2017-1125
MECHANICS OF HYBRID NANOCOMPOSITES: THE CARBON NANOTUBE/GRAPHENE EFFECT INTO FAILURE MODES

Suchilla G. Leão
Fernanda L R. Lima
Marina G. Martins
Nathalia C. Menezes
Matheus Norton
Universidade Federal de Minas Gerais, Mechanical Engineering Graduate Studies Program, 6627 Antonio Carlos Avenue, Belo Horizonte, MG 31270-901, Brazil
suchila.garcia@gmail.com, marinageorgiam@gmail.com

Antonio F Avila
Universidade Federal de Minas Gerais, Department of Mechanical Engineering, 6627 Antonio Carlos Avenue, Belo Horizonte, MG 31270-901, Brazil
avila@ufmg.br

Abstract. *This paper focuses on non-covalent functionalization of carbon nanotubes (CNT) and graphene GN) by employing non- and ionic surfactants. No changes on ultimate strength was noticed. The stiffness and failure strain were affected by the carbon based nanostructures dispersion. The increase Young's modulus was the same for GN and CNTs, around 9.0 %, but in different concentrations (GN 0.075 m/m % and CNT 0.15 m/m %). The increase on ID/IG peaks on Raman spectroscopy demonstrates a good interaction. The original GN ratio is around 0.17, the addition of CO890 lead to an aspect ratio of 0.26. For the CNT, the ID/IG ratio was equal to 1.0, and a moderate increase on ID/IG, i.e. 1.08 was noticed for CNT/SDBS. The FTIR analysis show a strong interaction for CNT/SDBS and GN/CO890. These interactions were accountable to the increase on energy required for breaking the nanostructures, which can be translated by an increase on stiffness and strength.*

Keywords: *Carbon fiber/epoxy laminates, graphene, carbon nanotubes, mechanical properties, FTIR analysis.*

1. INTRODUCTION

As discussed by Ávila et al. (2015), carbon based nanostructures, i.e. CNTs and graphene nanosheets, are promising as reinforcement for nanocomposites for aeronautical and aerospace applications, but the dispersion process and the cluster formation are problems to be overcome. To incorporate CNTs and graphene into composite materials, it is essential to achieve their stable suspension. As we know, carbon is a very active element, capable to produce various types of carbon allotrope. Graphene and carbon nanotubes (CNT) are two of these allotropes which present fascinating and unique properties due to the combination of the reduced dimensions and the different lattice structure. According to Zhu et al (2013), carbon has unique hybridization properties as a result of its structure capabilities to morphing due to changes in synthesis conditions. Among the most important carbon based nanostructures, carbon nanotubes (CNTs) and graphene nanosheets (GN) are truly the most important ones. Saito et al (2005) described carbon nanotube as a honeycomb lattice rolled into a cylinder. As debated by Carley et al (2013), carbon nanotubes have been the center of many researches due to their dimensions and remarkable electro-mechanical properties. In general, a CNT diameter has a nanometer size and its length can be more than 1μm. Its large aspect ratio (length/diameter) is appointed as one of the reasons for the CNTs notable properties, i.e. stiffness around 1.0 TPa and ultimate strength of approximately 160 GPa. The graphene mechanical properties are also comparable to the ones from the CNTs. As discussed by Kuilla et al. (2010), the tensile strength of graphene (130±10 GPa) is much higher than nano sized steel (1769 MPa), aramid fibers (3620 MPa) or natural rubber (20-30 MPa). These mechanical properties make graphene nanosheets and carbon nanotubes ideal nanostructures for nano-reinforcement of traditional high performance composites and in special carbon fiber/epoxy composites.

It is clear that CNTs and graphene nanosheets are promising as reinforcement for nanocomposites, but the dispersion process and the cluster formation are problems to be overcome. To incorporate CNTs and graphene into

composite materials it is essential to achieve their stable suspension. Due to the van der Waals forces between nanotubes and graphene sheets this structures have the tendency to form clusters/agglomerates. Although covalent chemical functionalization has been proposed to improve the dispersion of these carbon based nanostructures, this method could affect some of their properties. According to Bystrzejewski et al. (2010) as non-covalent modification is based on the adsorption of molecules onto the CNTs/graphene surface, their structures are not disturbed. To avoid graphene/CNT agglomeration Tkalya et al (2012) suggested the usage of surfactants. Therefore, a wide variety of surfactants have been studied and used for preparing stable dispersions of CNTs/graphene. As discussed by Tkalya et al. (2012), from a variety of surfactants, Sodium dodecyl benzenesulfonate (SDBS) and Polyoxyethylene Nonylphenyl ether (IGEPAL® CO-890) can be considered the most promising. As discussed by Pu et al. (2012), the use of surfactants is an approach capable of debundle CNTs and/or graphene and form a stable solution.

The main objective of this research is to investigate the effect of non-covalent functionalization by the usage of surfactant addition on carbon/epoxy composites nano-modified by carbon nanotubes and graphene.

2. MATERIALS AND EXPERIMENTS

To be able to understand the mechanisms behind the carbon based nanostructures and carbon fiber/epoxy composites a set of experiments was prepared. Notice that according to Silva Neto et al (2013) reported that the MLG dispersion into epoxy system has a saturation limit close to 2 m/m % and the optimum concentration for MWNT dispersion into epoxy systems seems to be around 0.30 m/m % stabilizing individual tubes without compromise its integrity and intrinsic properties. To be able to make a comparison between GN and CNTs the two carbon based nanostructures, this research employed the same concentrations. The hybrid carbon fiber/epoxy composite was prepared following three main steps.

First of all, the non-covalent functionalization process proposed by Avila et al. (2016) was implemented. CNTs and SDBS were dispersed into distilled water using a combination of sonication (42 KHz) and high shear mixer at 17400 RPM for one hour. The stable solution was dried in an oven for 24 hours. The same procedure was applied to GN and CO890. The surfactant concentrations were 200 ppm and 300 ppm for SDBS and CO890 respectively. Following the idea of design of experiments three different concentrations of GN and CNT were employed, i.e. low (0.075 m/m. %), a medium (0.15 m/m. %) and large (0.30 m/m. %). The following step was the non-covalent functionalized nanostructures dispersion into the epoxy system - a diglycidyl bisphenol A resin (AR300) and amine hardener (AH150) - from Barracuda Composites using a sonication bath system at 42 KHz for 30 minutes. The final step involved the carbon fibers – plain weave with areal density of 6 oz. /in^2, manual impregnation with cure on air for 24 hours and post-cure at 60 C for 8 hours. The 8 layers hybrid composites plates were cut with diamond saw and the tensile specimen were prepared following the ASTM D 3039 standard (2016). To be able to understand the carbon based nanostructures interactions with surfactants and with the epoxy/carbon fibers three different techniques were employed, i.e. Raman spectroscopy , Fourier Transformed Infra-Red Analysis (FTIR) and atomic force microscopy (AFM).

3. DATA ANALYSIS

The first set of experiments were based on interactions between the carbon based nanostructures, i.e. CNT and GN, and the surfactants. The idea behind these tests is to evaluate the non-covalent functionalization of those nanostructures. The functionalization will provide the necessary free radicals to allow the bonds between the epoxy system/carbon fibers and the nanostructures. As described by Avila et al. (2013) one powerful tool to measure the interactions between chemical specimens is the Fourier Transformed Infra-Red Analysis (FTIR). However, according to Ávila et al (2013), another technique which can be complementary to FTIR is the Raman spectroscopy. Therefore, the two techniques were employed. As were are dealing with two different carbon based nanostructures, i.e. CNT and GN, and two different surfactants, i.e. SDBS and CO890, it is clear that we have four different combinations (SDBS+CNT, SDBS+GN, CO890+CNT, CO890+GN). Figure 1 shows the FTIR signature for the surfactants and the specimen combinations.

According to Ju et al. (2012), the interaction between two substances (in our case, surfactant and carbon based nanostructures) can be identified by the presence of characteristic bands of the surfactant in the spectrum of functionalized nanostructures. The spectra of the surfactants and their characteristic bands are shown in FIGS. 1A and 1D. By analyzing the spectra of SDBS-functionalized nanostructures (FIG. 1B and 1C) the bands 2922 cm^{-1} and 2853 cm^{-1} (relative to the axial deformations of CH of aliphatic groups) characteristic of SDBS are identified for both the CNT and for GN functionalized by this surfactant. These bands are relative to the nonpolar portion of the surfactant and their presence in the functionalized nanostructured spectra indicates an interaction of this part of the molecule with the carbon nanostructures. It is also possible to observe that there was a decrease in the relative absorbance between these two bands when the nanostructures are mixed with the surfactant. According to Guo et al. (2014), changes in band intensity suggest a strong interaction between substances after mixing. In the case of SDBS+CNT the decrease in relative absorbance was higher than in SDBS+GN. These data indicate that both GN and CNT interacted with SDBS and that the affinity of this surfactant is higher with CNT than with GN.

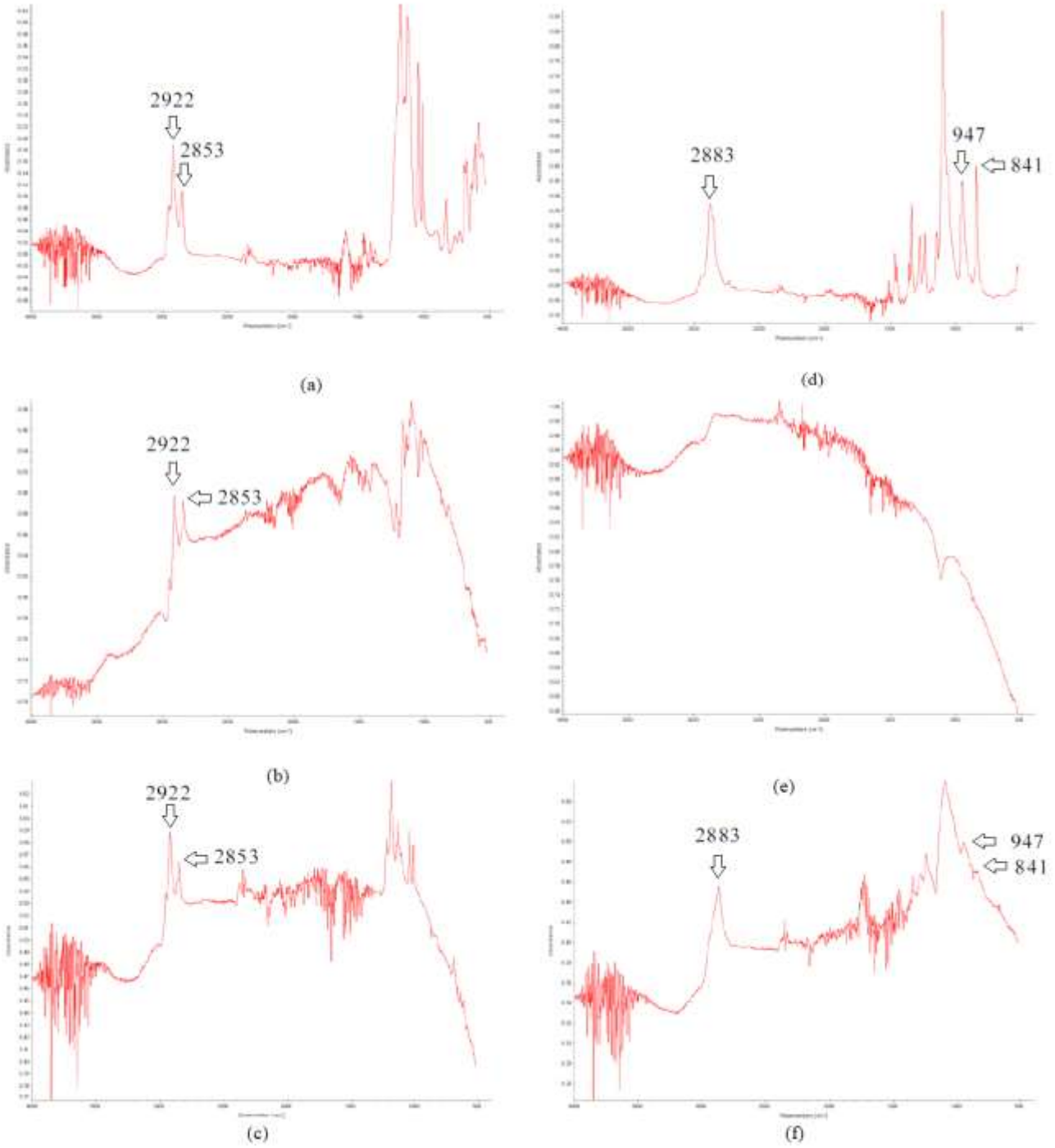

Figure 1. FTIR Signatures. (a) SDBS; (b) SDBS+CNT; (c) SDBS+GN; (d) CO890; (e) CO890+CNT; (f) CO890+GN

When the CO890 interaction was analyzed, a different scenario was observed. The CO890+CNT seem not have any interaction, as it can notice on FIG.1E, no CO890 characteristic band was identified into the functionalized specimen. The phenomenon is different when CO890+GN functionalized nanostructure, see FIG.1F, is analyzed. In this case, the 2883 cm^{-1} band (axial deformation of CH in alkanes), the 947 cm^{-1} band (stretch CO) and the 841 cm^{-1} band (adjacent 2H in an aromatic ring for -substituted), characteristics of the CO890 surfactant were observed. However, the relative absorbance was lower. This result indicates that there is an interaction of the apolar part of this surfactant with the GN nanostructure.

As commented by Englert et al. (2013), a single Raman spectrum can provide non-representative information of the sample analyzed, since the analysis is done locally and homogeneity at small scales is not always ensured. Therefore, the analysis was carried out at different points in the sample in order to have a representative results. The profile of the acquired spectra did not show significant variation and some of them are represented in FIG 2. In the

Raman spectra for the GN (FIG 2A) and the CNT (FIG 2D), it is possible to observe the bands characteristic to the sp^2 hybridized carbon structures. The band G at ≈ 1580 cm^{-1} corresponds to the stretch of the C-C link and the G 'band (also called 2D) at ≈ 2725 cm^{-1}, which according to Dresselhaus et al. (2010) is attributed to the second-order scattering involving two phonons, activated by the double resonance process. Note that according to Kim et al [16], in nano-crystalline samples or with imperfections in the structure, it is possible to observe the appearance of the D band at ≈ 1350 cm^{-1}. According to Englert et al. (2010), the D-band and exfoliation of the individual layers of graphene (2D band) were used to obtain information about the defects generated by sp3 (D-band) hybridization. For the GN spectrum (FIG 2A), it is possible to observe that graphene has more than one layer, since the G' band is wider and less intense than the G band. Englert et al. (2013) pointed out that an increase in the ID/IG ratio may be related to a satisfactory functionalization of the carbon nanostructures. The ID/IG ratios shown in FIG 2 are the mean of the values obtained in the different analyzes for each sample. It can be seen in the case of GN, the ID/IG ratio of 0.17 changed to 0.26 with CO890 functionalization and to 0.22 with SDBS. These values indicate that the functionalization of GN is more effective using CO890 than SDBS, a conclusion similar to that obtained in FTIR analysis. In the case of CNT, there is also an increase in the ID / IG ratio with the functionalization with both surfactants, however, it is observed in FIG 2E and 2F that the increase was greater for CO890 (1.08). Moreover, as discussed by Dresselhaus et al. (2010), the D band intensity is proportional to the sample atomic structure disorder. In FIG 2, it is possible to observe that there was an increase in the intensity of this band when both nanostructures were functionalized by the two surfactants, indicating a greater degree of disorder, which can be related to an effective functionalization.

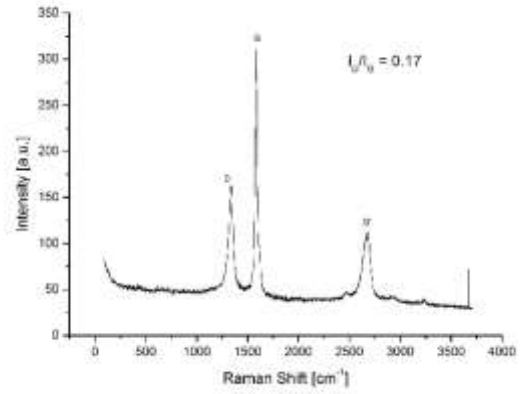

(a)

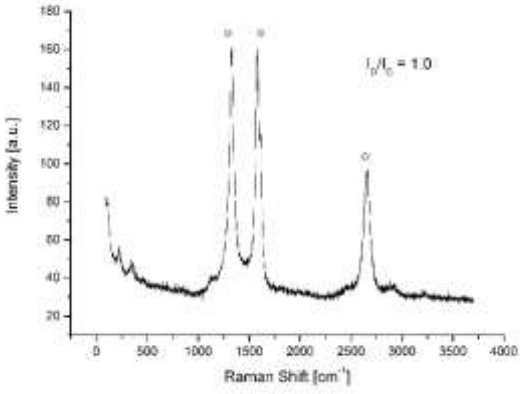

(d)

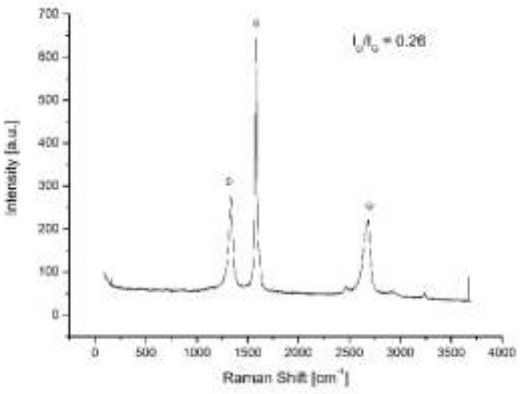

(b)

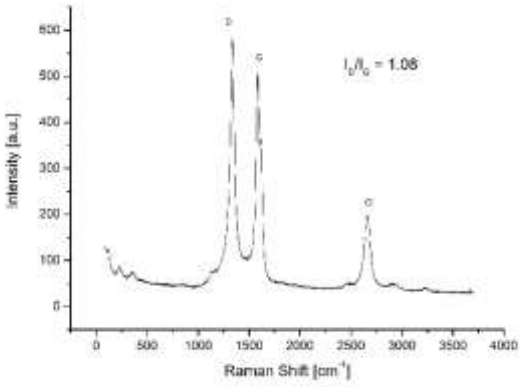

(e)

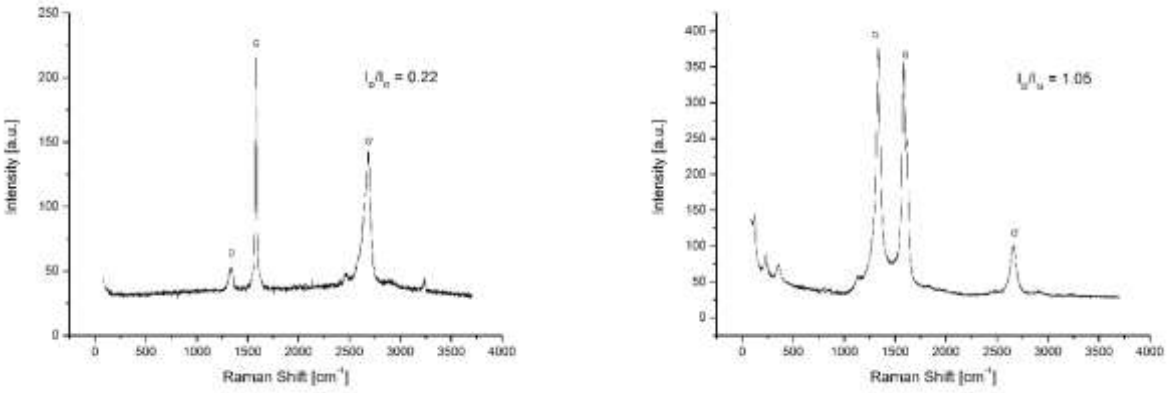

(c) (f)

Figure 2. Raman Spectra. (a) GN; (b) CO890+GN; (c) SDBS+GN; (d) CNT; (e) CO890+CNT; (f) SDBS+CNT;

As it can be observed by FTIR and Raman spectroscopy data each carbon based nanostructure has more affinity to individual surfactant. The best options are GN+CO890 and CNT+SDBS. The interaction between surfactant-carbon based nanostructures is an evidence of effective functionalization. A good functionalization can be translated into strong bonds at the fiber/matrix interface, in which can have direct influence into the overall mechanical properties. However, as the carbon based nanostructure concentrations were different, it is important to establish a relation between these concentrations and the nanostructure morphology formed during the dispersion process. Lee et al (2011) pointed out that these sub-micron nanostructures can affect the overall composite mechanical properties. Moreover, Shah and Batra (2014) went further, as they pointed that non-covalent functionalization has direct effect into nanostructure morphology. This new analysis must be performed using atomic force microscopy at sub-micron scale.

This analysis section focused on how the non-covalent functionalized carbon based nanostructure concentration affected the nanostructure morphology. As described early, three different concentrations of CNT/GN were tested, i.e. low (0.075 m/m. %), medium (0.15 m/m. %) and high (0.30 m/m %). After the non-covalent functionalization the CNTs/GNs were dispersed into the epoxy system, which was cure and post cure as in Avila et al. (2016). Figures 3 and 4 show the nanostructures formed for each group.

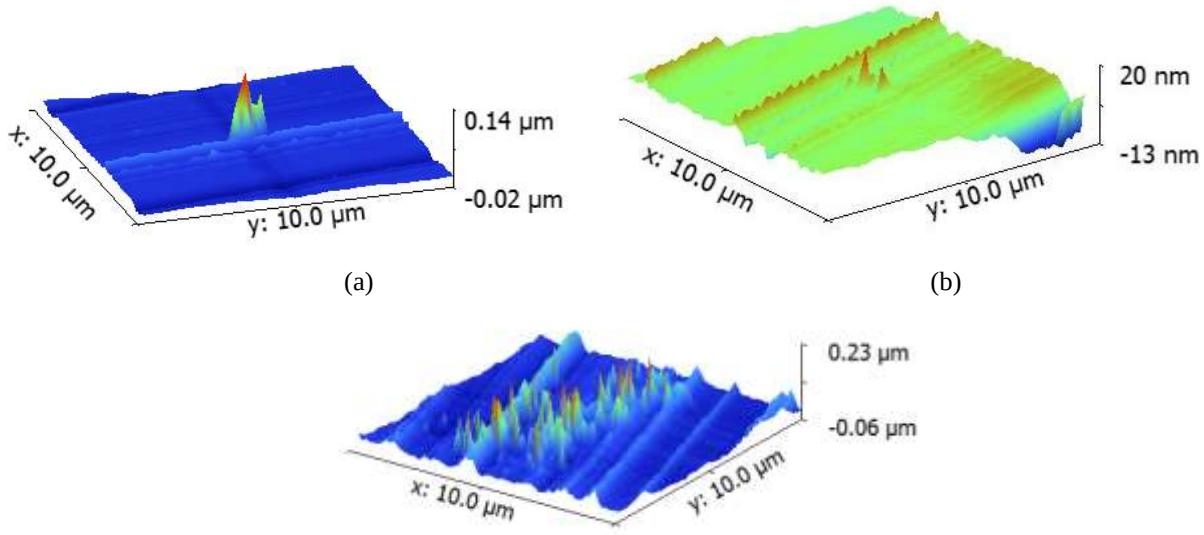

(a) (b)

(c)

Figure 3. AFM Observations. (a) 0.075 m/m % CNT; (b) 0.15 m/m % CNT; (c) 0.30 m/m % CNT

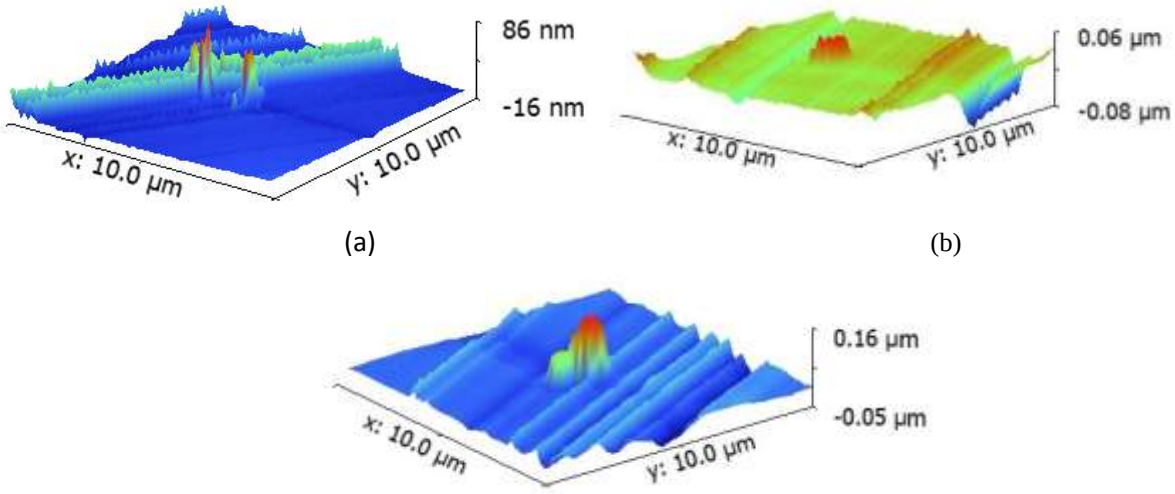

(a) (b)

(c)

Figure 4. AFM Observations. (a) 0.075 m/m % GN; (b) 0.15 m/m % GN; (c) 0.30 m/m % GN

As it can be noticed the CNT unidimensional nanostructure lead to a more uniform dispersion than the GN ones. In the CNT scattering distribution case, the 0.15 m/m % concentration (FIG. 3B) seems to have a wide spread condition. When this condition was compared against the 0.075 m/m % the peaks are much smaller, which can be an indication of more uniform distribution and a more intense interaction between CNT/SDBS/epoxy resin. In the case of GN, the two-dimensional nanostructure naturally lead to formation of tall and wide structures, which can be in some sense difficult to disperse, which can explain the more uniform distribution for the lowest concentration (FIG.4A). Finally, it is important to correlate the nanostructures formed and the overall composite mechanical behavior. The traditional tensile test is a good option for analyzing such correlation.

The tensile test was performed to allow us to evaluate at same time two important parameters, i.e. stiffness and the strength. Moreover, by observing the stress-strain curve it will be possible to exam each group mechanical response and make some numerical modeling predictions. Following ASTM D 3039 standard (2016) at least six samples were prepared and tested. Figures 5A-G show the stress-strain curves for the groups tested. Following the ASTM D 3039 standard, samples with fracture near the fixture were discarded. In all cases, at least five useful data were collected for each group.

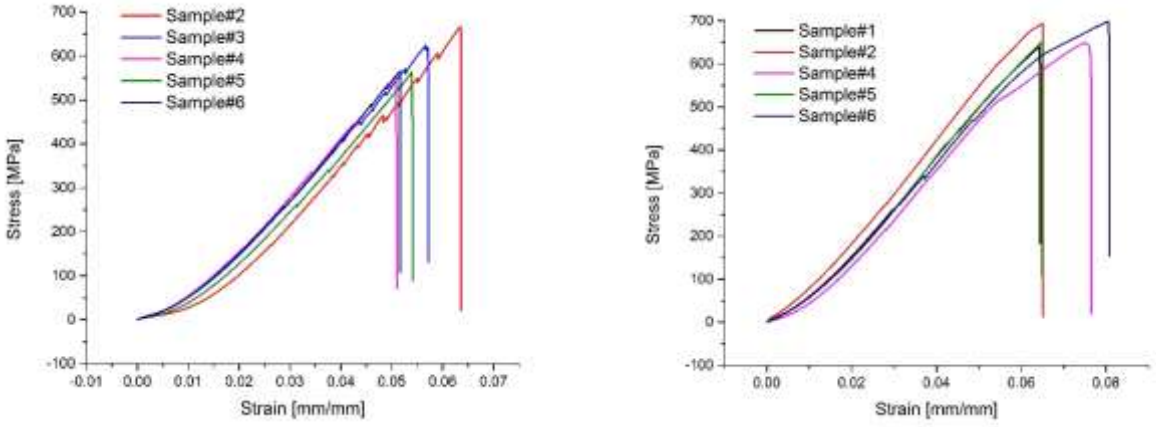

(a) (b)

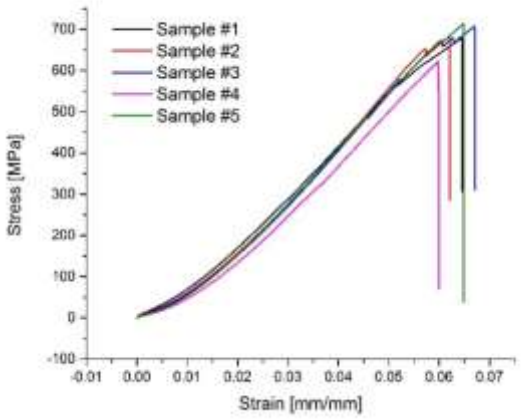

(c)

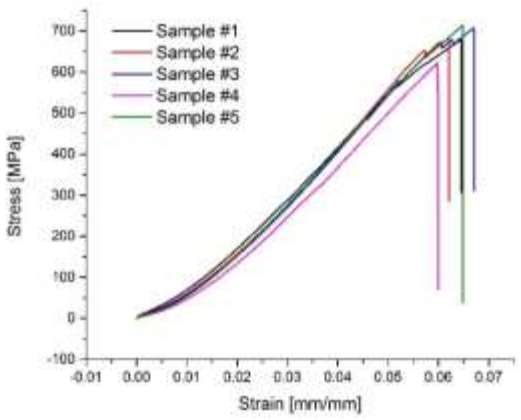

(d)

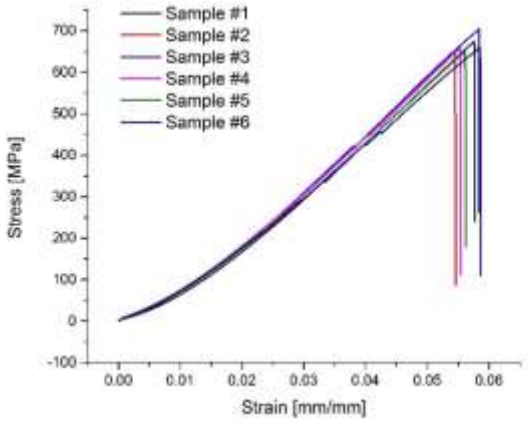

(e)

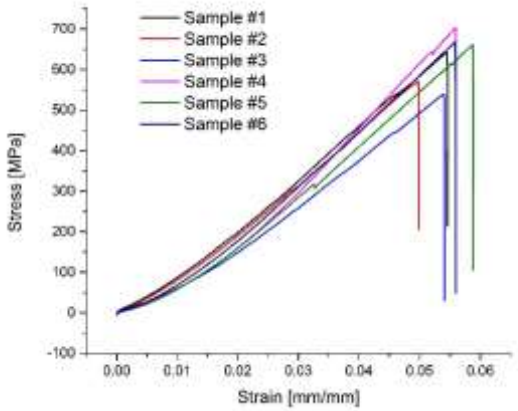

(f)

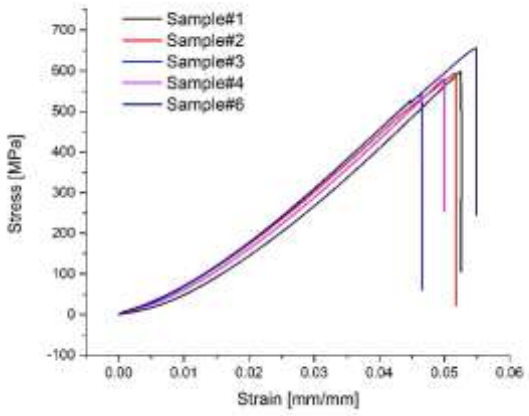

(g)

Figure 5: Tensile test stress-strain curves. (a) Control; (b) CNT 0.075 m/m %; (c) CNT 015 m/m %; (d) CNT 0.30 m/m %; (e) GN 0.075 m/m %; (f) GN 0.15 m/m %; (g) GN 0.30 m/m %.

Figure 5A represents a near linear stress-strain curve, which was expected for a carbon/epoxy composite. The CNT addition seems to affect the stress-strain curve, as they appear to be elastic-plastic like shape. This behavior can be

due to the CNT interlocking effect. When the stress reaches values around 600 MPa, see FIGs 5B-D, this storage energy is released and there is a decrease on stiffness (decrease on slope). The GN effect seems to be broader as no substantial changes on initial stiffness were noticed (FIG. 5E-G). However, some decrease on stresses are observed, which can be described as shear failure of nanostructures formed. This hypothesis is based on the applied force and the assumption that these nanostructures were perpendicular to the applied load. Table 1 summarizes the key parameters, i.e. stiffness, ultimate strength and strain at failure, for each group tested. A statistical analysis was performed and, at 95% level of confidence, the ultimate strength seems to be not affected by neither CNT nor GN. This seems to indicate that strength is fiber dominated. When stiffness is evaluated the results were different. The Young's modulus were significant different in all cases, which can lead to the conclusion that stiffness is matrix dominated. The biggest increase on stiffness, around 8.5%, seems to be due to the graphene (GN 0.30 m/m %) addition. This phenomenon could be explained by the "extra" grip provided by the GN nanostructures at the fiber/resin interface as explained by Mittal (2014) and Avila et al. (2012).

Table 1 Tensile tests summary

Group ID	Ultimate Strength [MPa]	Strain at Failure [mm/mm]x10^{-2}	Stiffness [GPa]
Control	593.923±47.936	5.544±0.521	12.980±0.670
CNT075	666.165±27.951	7.006±0.748	10.929±0.354
CNT015	680.864±36.147	6.373±0.279	11.985±0.391
CNT030	650.114±71.082	5.704±0.352	12.942±0.722
GN075	666.318±20.694	5.676±0.169	13.295±0.417
GN015	630.377±63.859	5.479±0.301	12.968±1.719
GN030	595.534±40.299	5.104±0.313	13.878±0.367

4. CONCLUSIONS

From the strength point of view, no significant changes were notice, however, stiffness and failure strain were affected by the carbon based nanostructures dispersion. The increase Young's modulus was approximately the same for GN and CNTs, i.e. around 8.5%, but in different concentrations (GN 0.075 m/m % and CNT 0.15 m/m %). This phenomenon can be explained by the Raman spectroscopy associated to the FTIR and the AFM. The increase on ID/IG peaks on Raman spectroscopy is an evidence of good interaction. The original GN ration is around 0.17, the addition of CO890 lead to an aspect ratio of 0.26. For the CNT used in this research, the ID/IG ratio was equal to 1.0, and a moderate increase on ID/IG, i.e. 1.08 was noticed with the usage of SDBS. In all cases, the interactions between CNTs/GNs and surfactants were improved. The FTIR analysis show a strong interaction between the SDBS and CNT (peaks 2922 and 2853 cm-1) and between the CO890 and GN (peaks 2883, 947 and 841 cm^{-1}). These interactions can be "translated" as formation of nanostructures that are responsible to the increase on energy required for breaking these nanostructures, which can be translated by an increase on stiffness.

5. ACKNOWLEDGMENTS

The authors would like to acknowledge the financial support provided by the Brazilian Research Council (CNPq) under grant 304646/2014-8 and the Air Force Office of Scientific Research (AFOSR) grant FA9550-14-1-0377. We also would like to acknowledge the technical support provided by the UFMG's Center for Micro-Analysis and the Minas Gerais State Foundation for Research (FAPEMIG).

6. REFERENCES

ASTM D 3039M. 2016. "Standard Test Method for Tensile Properties of Polymer Matrix Composite Materials", *ASTM Annual Book of Standards*, Vol. 15.03, p. 1-13.

Ávila, A.F., V.C. Munhoz, A.M. de Oliveira, M.C.G. Santos, G. R.B.S. Lacerda, C. F. Gonçalves. 2014. "Nano-based systems for oil spills control and cleanup". *J. of Hazardous Materials*. Vol. 272, p.20-27.

Ávila, A.F., Munhoz, V.C., Menezes, N.C., da Silva, C.F., Leão, S.G. 2016. "Non-covalent functionalisation of carbon-based nanostructures and its application to carbon/epoxy composites". *Int. J. of Nanotechnology*, Vol. 13, p. 573-584.

Ávila, A.F., Silva Neto, A., Nascimento Jr. H. 2011. "Hybrid nanocomposites for mid-range ballistic protection" *International Journal of Impact Engineering*, Vol. 38, p. 669-676.

Bystrzejewski, M., Huczko, A., Lange, H., Gemming, T., Büchner, B. and Rümmeli, M.H. 2010. "Dispersion and diameter separation of multi-wall carbon nanotubes in aqueous solutions", *J. Colloid Interface Sci.*, Vol. 345, p.138–142.

Carley, G., Moraes, V.G., Ávila, A.F. and Oliveira, S. 2013. "Nano-engineered composites: interlayer carbon nanotubes effect", *Materials Research*, Vol. 16, p.628–634.

Dresselhaus, M.S., Jorio, A., Hofmann, M., Dresselhaus, G., Saito, R. 2010. "Perspectives on carbon nanotubes and graphene Raman Spectroscopy", *Nano Letters*. Vol.10, p.751-758.

Englert, J.M., Vecera, P., Knirsch, K.C., Shafer, R.A., Hauke, F., Hirsch, A. 2013. "Scanning-Raman-Microscopy for the statistical analysis of covalently functionalized graphene", *American Society of Chemistry Nano*. Vol.7, p.5472-5482.

Guo, Z., Wang, S., Wang, G., Niu, Z., Yang, J., Wu, W. 2014. "Effect of oxidation debris on spectroscopic and macroscopic properties of graphene oxide", *Carbon*, Vol.76, p.203-211.

Ju, L., Zhang, W., Wang, X., Hu, X., Zhang, Y. 2012. "Aggregation kinetics of SDBS-dispersed carbon nanotubes in different aqueous suspensions", *Colloids and Surfaces A: Physicochemical and Engineering Aspects*. Vol.409, p.159-166.

Kim, Y.A., Fujisaka, K., Muramatsu, H., Hayashi, H., Endo, M., Fujimori, T., Kaneko, K., Terrones, M., Behrends, J., Eckmann, A., Casiraghi, C., Novoselov, K.S., Saito, R., Dresselhaus, M. 2012. "Raman Spectroscopy of boron-doped single-layer graphene", *American Society of Chemistry Nano*. Vol.6, p.6293-6300.

Kuilla, T., Bhadra, S., Yao, D., Kim, N.H., Bose, S. and Lee, J.H. 2010. "Recent advances in graphene based polymer composites", *Progress in Polymer Science.* Vol. 35, p.1350–1375.

Pu, N-W., Wang, C-A., Liu, Y-M., Sung, Y., Wang, D-S. and Ger, M-D. 2012. "Dispersion of graphene in aqueous solutions with different types of surfactants and the production of graphene films by spray or drop coating", *J. Taiwan Inst. Chem. Eng.*, Vol. 43, p.140–146.

Saito, R., Dresselhaus, G. and Dresselhaus, M.S. 2005. *Physical Properties of Carbon Nanotubes*, Chapter 3, Imperial College Press, London, UK.

Silva Neto, A., da Cruz, D.T.L., Ávila, A.F. 2013. "Nano-modified Adhesive by Graphene: The Single Lap-Joint Case', *Materials Research*, Vol.16, p. 592-596.

Tkalya, E., Ghislandi, M., de With, G. and Koning, C.E. 2012. "The use of surfactants for dispersing carbon nanotubes and graphene to make conductive nanocomposites", *Current Opinion Colloid Interface Sci*., Vol. 17, p.225–232.

Zhu, J., Chen, M., He, Q., Shao, L., Wei, S. and Guo, Z. 2013. "An overview of the engineered graphene nanostructures and nanocomposites", *Royal Society of Chemistry Advances*, Vol. 109, p.22790–22824.

7. RESPONSIBILITY NOTICE

The last author is the only responsible for the printed material included in this paper.